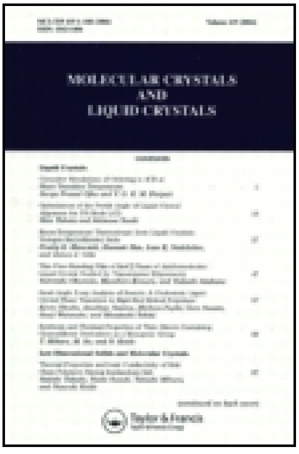

Molecular Crystals and Liquid Crystals
Publication details, including instructions for authors and subscription information:
http://www.tandfonline.com/loi/gmcl18

Simulation of Two-Dimensional Nematic Director Structures in Inhomogeneous Electric Fields

Gunther Haas [a], Henning Wöhler [a], Michael W. Fritsch [a] & Dieter A. Mlynski [a]

[a] Institut für Theoretische Elektrotechnik und Meßtechnik, Universität Karlsruhe, Kaiserstr. 12, D-7500, Karlsruhe, W. Germany

Version of record first published: 24 Sep 2006.

To cite this article: Gunther Haas, Henning Wöhler, Michael W. Fritsch & Dieter A. Mlynski (1991): Simulation of Two-Dimensional Nematic Director Structures in Inhomogeneous Electric Fields, Molecular Crystals and Liquid Crystals, 198:1, 15-28

To link to this article: http://dx.doi.org/10.1080/00268949108033379

Mol. Cryst. Liq. Cryst., 1991, Vol. 198, pp. 15–28
Reprints available directly from the publisher
Photocopying permitted by license only

Printed in the United States of America

Simulation of Two-Dimensional Nematic Director Structures in Inhomogeneous Electric Fields

GUNTHER HAAS, HENNING WÖHLER, MICHAEL W. FRITSCH and DIETER A. MLYNSKI

Institut für Theoretische Elektrotechnik und Meßtechnik, Universität Karlsruhe, Kaiserstr. 12, D-7500 Karlsruhe, W. Germany

(Received July 26, 1990)

We have developed a numerical method for the calculation of the two-dimensional director distribution of nematic liquid crystals in inhomogeneous electric fields which is able to handle solutions with disclinations. As an application we firstly study the formation of disclinations in liquid crystal displays with small pixel electrodes due to the inhomogeneous electric field near the edges of the electrodes. Secondly we analyze in detail the director structure and the optical properties of a cylindrical liquid crystal microlens consisting of a liquid crystal cell with a slit patterned electrode in order to create an inhomogeneous electric field. Results for the focal length and the focussing quality as a function of the applied voltage and the width of the slit are given.

Keywords: simulation, nematic liquid crystals, disclinations, liquid crystal microlens

1 INTRODUCTION

If the size of the electrode structure in a liquid crystal (LC) cell becomes comparable to the cell thickness, effects due to the inhomogeneous electric field have to be considered. This concerns e.g., light valves for screen projection systems because of their limited overall size or active addressed (TFT) LC-Displays (LCDs) because of their narrow signal electrodes. Additionally, two-dimensional LC structures play an important role for some recently developed LC devices based on Fourier optics, e.g. LC lenses[1,2] or LC phase modulators.[3]

Two main effects causing the formation of two-dimensional LC structures have to be considered: Firstly, the electric field near the edges of an electrode becomes inhomogeneous and penetrates into the region outside the electrode within a spatial range comparable to the cell thickness. Secondly, there are elastic forces acting parallel to the cell boundaries which must be considered.

On one hand, these effects influence the electro-optical properties of the cell, on the other hand they induce an inhomogeneous LC structure between two adjacent pixels (meshing), the latter reducing the spatial resolution of an LCD. For the LC-microlens[1] mentioned above this inhomogeneous structure is used for creating a lenslike refractive index profile. Additionally, the electric field near the edges is oblique with respect to the cell boundaries thereby prescribing a fixed direction for the tilting of the LC structure which, together with the elastic forces, can favour the formation of so called disclinations. Disclinations are discontinuities in the local molecular alignment and can be seen as threadlike regions.

In order to get insight into these effects we have developed a numerical method to calculate the LC orientation and the corresponding electric field distribution in two-dimensional electrode structures, where the interaction between nematic director and electric field and vice versa has been taken fully into account.[4] Furthermore, by starting from a tensor formulation[5] of the equations of continuum theory in order to describe the correct nematic director symmetry, we are able to obtain solutions involving disclinations.

This method has been successfully applied to the calculation of the electro-optical properties of parallel and homeotropically aligned and twisted nematic (TN) LCDs with small pixel electrodes.[4,6,7] In this paper we will shortly summarize the most important effects for LCDs and present results for the LC-microlens.

2 THEORY

A typical two-dimensional geometry is shown in Figure 1. It consists of a single stripe electrode with an applied voltage U opposite to a ground electrode of infinite size. The arrangement is assumed to be of infinite size in the z direction, therefore all functions depend only on x and y. The region between $y = 0$ and $y = d$ is filled with liquid crystal material, above $y = d$ there is an isotropic region. This example is a two-dimensional cross-section through a pixel in an LCD.

2.1 Electric Field

In order to calculate the electric field distribution $\mathbf{E}(x,y)$ we have to solve the potential equation which becomes in our case:

$$\begin{aligned} \left(\epsilon_\perp + \Delta\epsilon\, n_x^2\right) \frac{\partial^2}{\partial x^2}V + \left(\epsilon_\perp + \Delta\epsilon\, n_y^2\right) \frac{\partial^2}{\partial y^2}V & \\ +2\Delta\epsilon\, n_x n_y \frac{\partial^2}{\partial x \partial y}V & \\ +\Delta\epsilon \left(2n_x\frac{\partial n_x}{\partial x} + n_x\frac{\partial n_y}{\partial y} + n_y\frac{\partial n_x}{\partial y}\right)\frac{\partial}{\partial x}V & \\ +\Delta\epsilon \left(2n_y\frac{\partial n_y}{\partial y} + n_y\frac{\partial n_x}{\partial x} + n_x\frac{\partial n_y}{\partial x}\right)\frac{\partial}{\partial y}V & = 0, \qquad \mathbf{E} = -\mathbf{grad}V. \end{aligned} \tag{1}$$

Here $V(x,y)$ is the electrostatic potential function, $\epsilon_\perp$ is the dielectric constant perpendicular with respect to the director and $\Delta\epsilon$ is the dielectric anisotropy. For $\Delta\epsilon << \epsilon_\perp$ Equation (1) reduces to the Laplace equation and the electric field is independent of the director field. However, this condition is not fulfilled for nematic liquid crystals because their dielectric anisotropy is rather large. Equation (1) is linear in the potential function V but depends nonlinearily on the nematic director field.

2.2 Director Field

In two-dimensional director structures there are often solutions which involve disclinations. These cannot be described by the usual nematic continuum theory, where the equations for the local molecular orientation are expressed in terms of the unit vector field $\mathbf{n}(x,y)$. Consider e.g. the director field shown in Figure 2. It shows the two possible ground states of a so called π-cell. The two states are separated by a disclination-line perpendicular with respect to the plane located in the center. Due to the rotation of the director around the disclination there are points where adjacent directors are antiparallel to each other, which results in a physically senseless singularity of the director field. At the center of the disclination two adjacent directors are perpendicular to each other. From nematic symmetry it follows, that this should be a metastable state if only the two neighbours are considered, whereas in the vector formulation there is always a gradient of energy forcing adjacent directors to align parallel to each other. It is therefore obvious that a vector field is not an adequate object to describe mathematically the nematic orientation, because in this description $\mathbf{n}$ and $-\mathbf{n}$ are not equivalent as required by the nematic symmetry.†

A numerical method for the calculation of director structures which takes into account the nematic symmetry was recently developed.[5] It starts from a reformulation of the equations of continuum theory in terms of an alignment tensor with the correct symmetry properties. In this representation, the equation for the relaxation of the director field, neglecting backflow and in one-constant approximation, is

$$\gamma_1 \frac{\partial}{\partial t} n_i n_j = k\left(\frac{\partial^2}{\partial x^2} + \frac{\partial^2}{\partial y^2}\right) n_i n_j + \Delta\epsilon\, \overleftrightarrow{E_i E_j} + \lambda n_i n_j, \qquad \sum_{i=1}^{3} n_i n_i = 1. \tag{2}$$

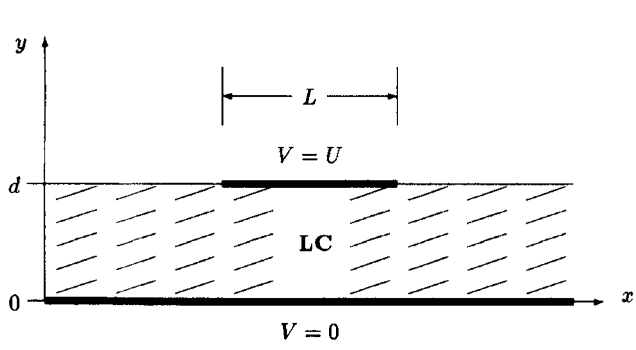

FIGURE 1 Two-dimensional geometry of stripe electrode.

† Originally, from the existence of disclinations the nematic symmetry was deduced.

Here, n_i are the cartesian components of the nematic director, γ_1 is the rotational viscosity coefficient and k the Frank elastic constant. We have already considered the constraint by adding the corresponding force term $\lambda n_i n_j$ in Equation (2), where the function $\lambda(x,y)$ is a Lagrange Multiplier.

2.3 Numerical Method

In order to solve the nonlinearily coupled set of partial differential equations (PDE) we applied a finite difference (FD) method.[8] For spatial discretization the region of interest is covered with a FD-grid. Substituting all functions by the set of their node variables and replacing all differential operators by discretized expressions we get from a PDE a large set of ordinary equations in the node variables which is solved numerically.

For the director field we firstly perform the spatial discretization of the tensorial Equation (2) and afterwards the projection onto the vector representation by multiplying the discretized equation by $\mathbf{n}$. This procedure leads to an algorithm where the nematic symmetry is preserved.[5]

It should be noted here that for the formation of a disclination, as e.g. shown in Figure 2, where large distortions between adjacent directors occur, our numerical model can in general give only qualitative results due to the different size and energy between the simulated and the real disclinations. In our simulation the size of the disclination is comparable to the grid spacing, whereas the core of a real disclination is rather within the range of molecular dimensions. Therefore the energy of the disclinations in our model might be different from real ones. However, the correct grid spacing can be adjusted by comparison with experiments.

Our algorithm works as follows: We assume an initial director configuration $\mathbf{n}(x,y)$ to be given at time $t = 0$. From this we firstly calculate the corresponding electric field by solving the discretized form of Equation (1) as described above. Integration in time of Equation (2) is performed by an alternating direction implicit (ADI) method[8] which we modified for the constraint. After each timestep the electric field is computed from the new director field. Iteration is performed until a steady state is reached.

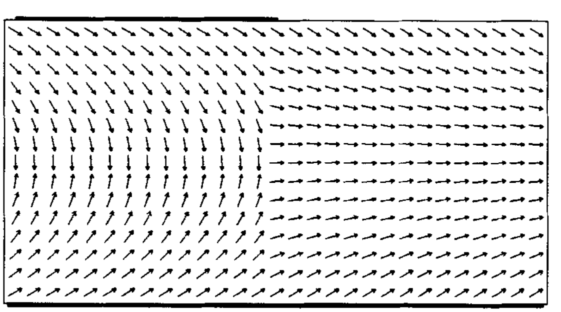

FIGURE 2 Director field of a line disclination in a π-cell.

3 RESULTS

3.1 Narrow Stripe Electrode

As a model for a pixel in an LCD we consider the geometry of a single stripe electrode as shown in Figure 1, with the ratio of the width of the stripe over the cell thickness, L/d, as a parameter. We assume the LC to be aligned in the x-y plane with a small pretilt angle θ_0 of typically a few degrees with respect to the x-axis (parallel alignment).

The properties of this configuration have been studied in detail in Reference 6. There we found, in accordance with experimental observations, that the most significant effect of the small pixel electrodes is the so called reverse tilting of the director structure due to the inhomogeneous electric field near the edges of the electrode. This means that the pixel is divided into two domains with an oppositely tilted director distribution. Below some critical voltage U_c, which turns out to be approximately 1.5–2 times the Fredericks voltage, the two domains are separated by a layer with parallel alignment known in the literature as bend wall. Above U_c the bend wall breaks up into two line disclinations connected by a layer with homeotropic alignment which is called a reverse tilt disclination. This holds even if we apply a pretilt angle at the boundaries. The effect of the pretilt is mainly to shift the location of the bend wall or the disclination, respectively, towards one

$U < U_c$

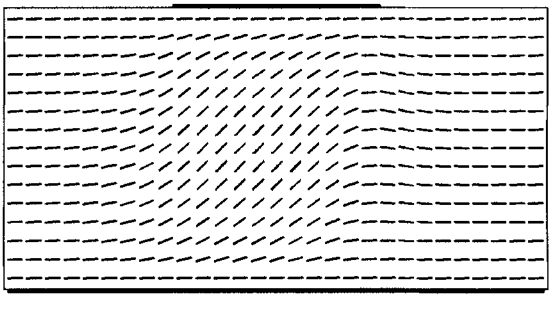

$U > U_c$

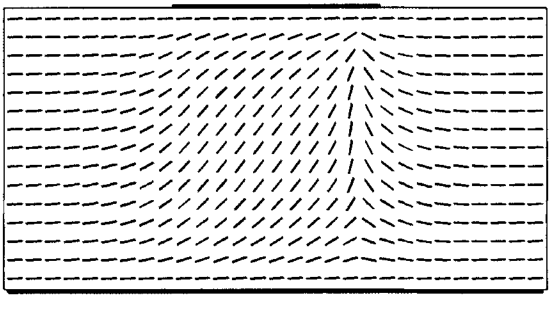

FIGURE 3 Director distribution below and above U_c, $L/d = 4$, $\theta_0 = 2°$. The vertical axis is stretched by a factor of 4.

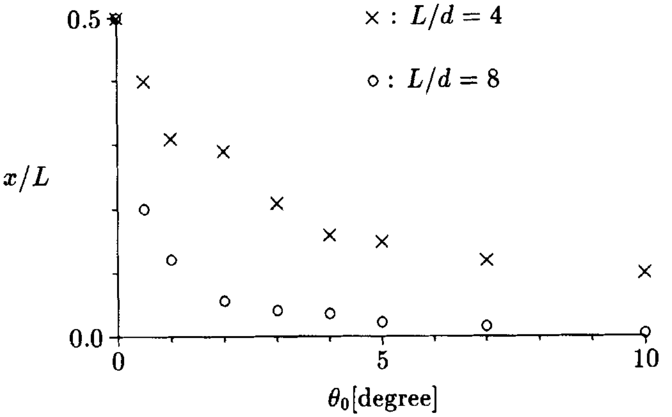

FIGURE 4 Location of the disclination as a function of pretilt angle θ_0. $x/L = 0$ corresponds to the edge and $x/L = 0.5$ to the center of the electrode.

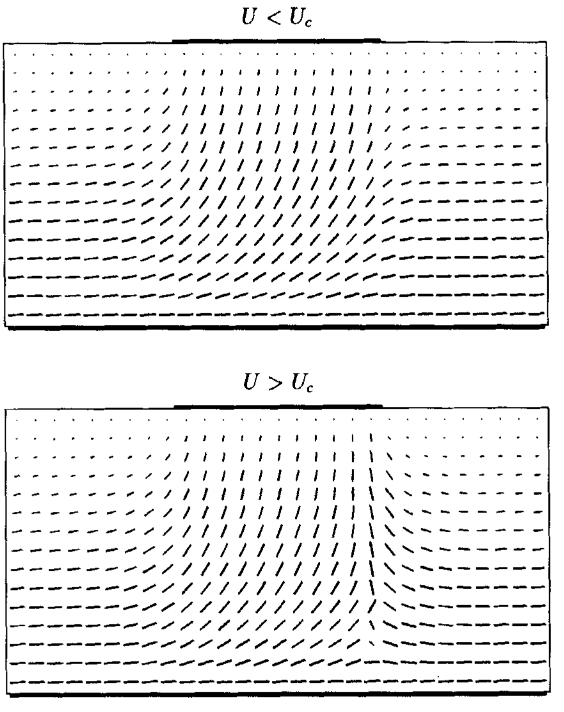

FIGURE 5 Director distribution of a TN-LCD with alignment parallel to the stripe below and above U_c, $L/d = 4$, $\theta_0 = 2°$. The vertical axis is stretched by a factor of 4.

edge of the electrode. Because of this, the optical appearance of a single pixel is considerably influenced by the reverse tilting only if the size of the electrode is smaller than approximately 8 times the cell thickness, if we assume a pretilt angle of a few degrees as typical for parallel aligned LCDs. The director distribution

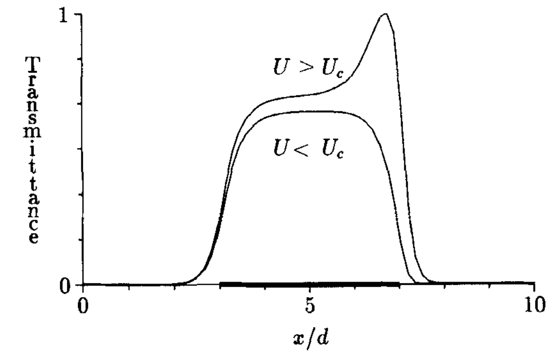

FIGURE 6 Transmittance over pixel for the TN-LCD, voltage below and above U_c, $\Delta nd = 0.5$, $L/d = 4$, $\theta_0 = 2°$. The location of the electrode is marked on the x-axis.

below and above U_c are shown in Figure 3. Figure 4 shows the location of the disclination on the pixel as a function of the pretilt angle.

The behaviour of a homeotropically aligned LCD with the pretilt angle in the x-y plane is qualitatively the same and is studied in detail in Reference 6. The main difference to the parallel alignment is that we now have relatively small pretilt angles necessary for a homeotropically aligned LCD.[9] Due to the rather small pretilt angle the disclination is located more distant with respect to the edge of the electrode and is therefore visible for larger L/d-ratios.

A 90° twisted (TN) LCD shows principally the same behaviour like the parallel aligned. Figure 5 shows the director distribution below and above the critical voltage for a TN-LCD with the alignment being parallel with respect to the stripe. If the alignment is oblique with respect to the stripe as usual for LCDs because this offers the best viewing angle dependence, the formation of the disclination is favoured which means that the critical voltage is lowered. Additionally, if the mid-plane director is perpendicular with respect to the x-y plane the oblique electric field causes a reversing of the sense of rotation of the helix. This is studied in detail in Reference 7. Figure 6 shows the transmittance over x for the TN-LCD calculated with the Jones matrix method[10] assuming normal incidence.

3.2 LC-Microlens

The recently presented LC-microlens[1] consists of a parallel aligned LC-cell with a hole patterned electrode of 750 μm in diameter on one side and a transparent counter electrode on the other side. The idea is, that because of the inhomogeneous electric field due to the hole we will get LC structure which is inhomogeneously deformed in direction parallel to the cell boundaries. For incident light with its polarization parallel with respect to the director at the boundaries, this structure can produce a phase-profile similar to that of a lens so that a light beam can be focussed. The focal length of the device can be controlled by the voltage applied on the electrode. In Reference 1 it was shown experimentally, that such a device possesses focussing properties, and that at a relatively high voltage it changes into a diverging lens.

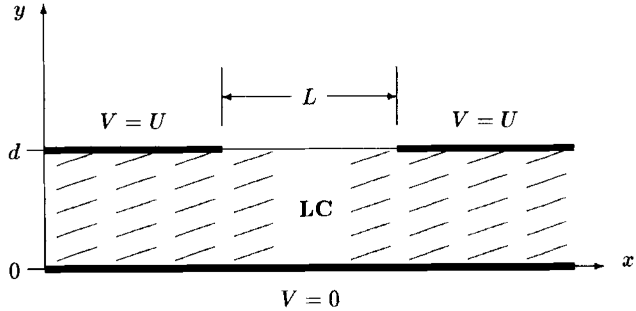

FIGURE 7 Slit geometry for the cylinder-microlens.

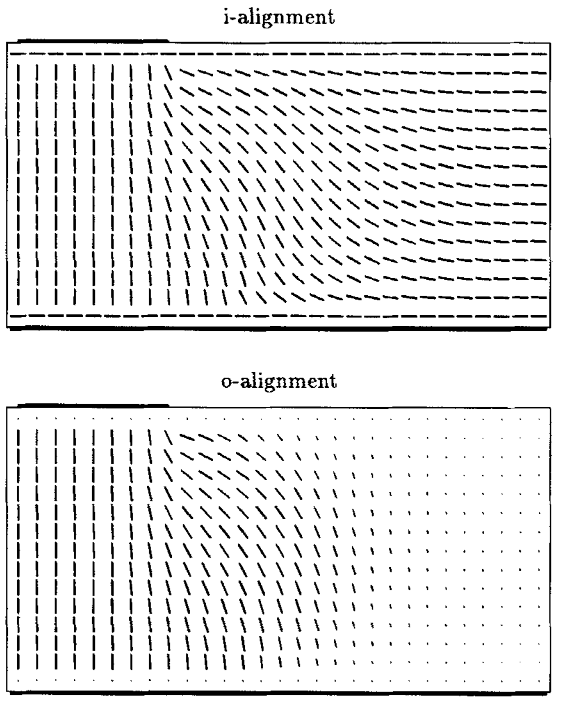

FIGURE 8 Director distribution of the LC-microlens for the two kinds of alignment, $L/d = 10$, $U = 14$.

We now want to analyze these properties with our numerical model. Unfortunately the axial symmetry of the geometry is destroyed by the unidirectionally aligned LC which lowers the achievable focussing qualities of the lens. Instead of solving the 3-dimensional problem of the circular hole we therefore restricted to the case of a cylindrical lens which can be created by an electrode with a rectangular slit. The geometry of the slit-configuration is shown in Figure 7 where we introduce the parameter L/d which is the ratio of the width of the slit to the cell thickness and the voltage U, given in units of the Fredericks-voltage. We considered two different kinds for the alignment at the boundaries: The director can be either *in*

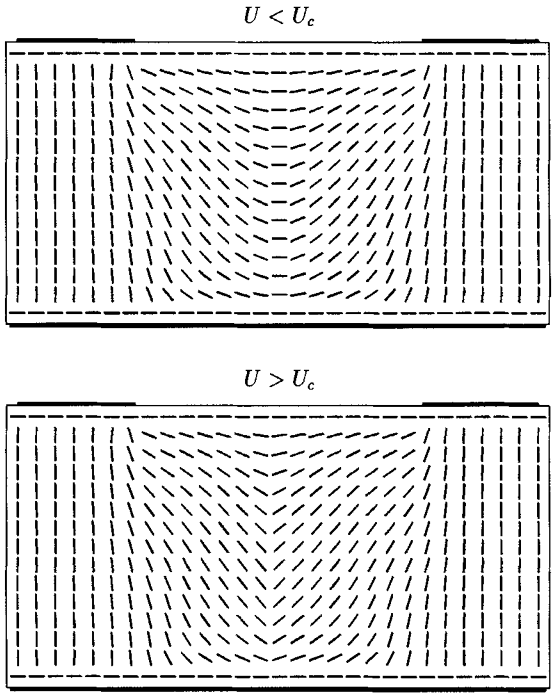

FIGURE 9 Director distribution for the i-alignment below and above U_c, $L/d = 5$, $U_c = 7$.

the *x-y* plane (i-alignment) or *out of* the *x-y* plane (o-alignment). This can also be considered as an approximation for two mutually perpendicular cross-sections through the hole patterned electrode. However, a hole of certain diameter L does not correspond to a slit of the same width L because inside the hole the electric field strength is larger compared to the slit. Our results therefore correspond to a hole with a larger diameter.

In Reference 1 the ratio of the hole diameter to the cell thickness is 15. We have made calculations for L/d-ratios of 5, 10 and 15. Because of the symmetry of the arrangement we have to perform the calculations only in half of the region of Figure 7 because we applied Neumann boundary conditions at the left and right boundary which means $\partial \mathbf{n}/\partial x = 0$ there. Therefore all following figures except Figure 9 show also only the half of the region of Figure 7. Figure 8 shows the director distributions for an L/d-ratio of 10. The behavior of the two kinds of alignment is quite different: In case of the i-alignment we have a pure bend/splay deformation and the director remains in the *x-y* plane whereas in case of the o-alignment we have mixed bend/splay/twist deformation due to the oblique electric field. At a relatively large voltage we have the formation of a disclination in the center similar to the reverse tilt disclination in case of the stripe electrode for the i-aligned case as shown in Figure 9. The orientation in the center thereby changes from parallel to homeotropic. This will create a phase-profile which has defocusing properties as observed experimentally. For L/d-ratios of 10 and 15 the disclination does not occur at reasonable voltages because the field in the center is not large enough to induce the disclination.

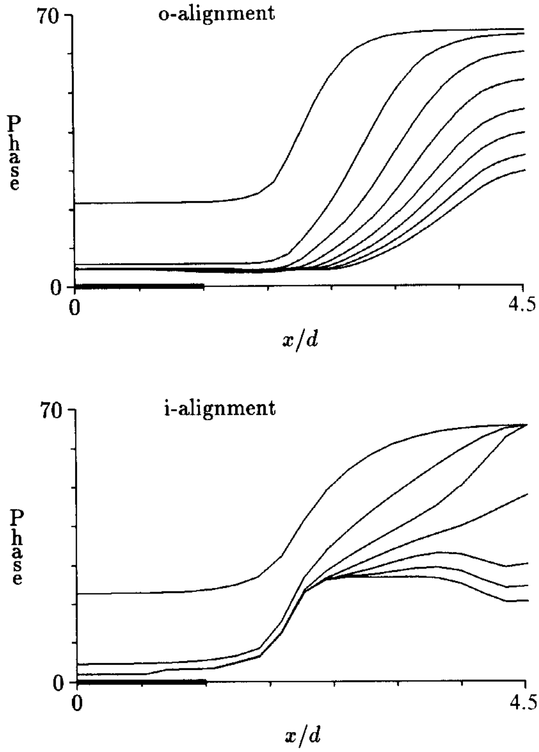

FIGURE 10 Phase-profiles (in°/μm) for o- and i-alignment, $L/d = 5$, $U = 2, 4, 6, 8, 10, 12, 14$ (from left to right) $\Delta n = 0.1$. The location of the electrode is marked on the x-axis.

In the o-aligned case the disclination does not occur because the director in the center tilts unidirectionally out of the x-y plane.

Next we calculated the phase-profile for normally incident light with its polarization parallel to the director at the boundaries. The phase-profiles were calculated with the help of the Jones matrix method,[10] neglecting a possible influence of the variation of the refractive index in x-direction on the light propagation. They are shown in Figures 10 and 11 for L/d-ratios of 5 and 10, respectively. The profiles for the i- and o-alignment at the same voltage are different because of two reasons: Firstly, we have a mixed deformation in case of the o-alignment as discussed above. Secondly, in case of the o-alignment we have a coupling of the two optical modes whereas in case of the i-alignment we only have the extraordinary mode. It is therefore obvious that the hole patterned electrode device cannot possess cylindrical symmetry. Additionally, for an L/d-ratio of 5 the disclination occurs above some voltage for the i-alignment.

A lenslike phase-profile which should be a quadratic function in x can only be created for an L/d-ratio equal or less than 10. For $L/d = 15$ the profiles are essentially the same as shown in Figure 11 for $L/d = 10$ but with a large plateau in the center. This plateau cannot be avoided by applying a higher voltage because then the whole curves are shifted towards the center so that the effective aperture is reduced. However this result cannot be directly applied to the hole patterned

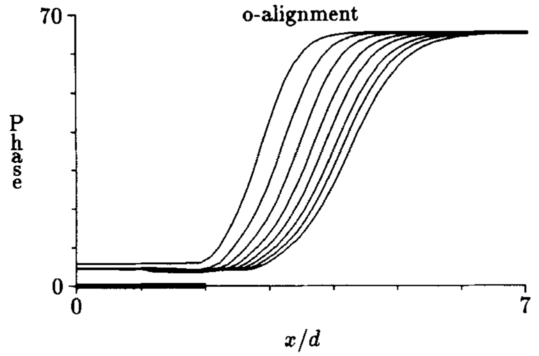

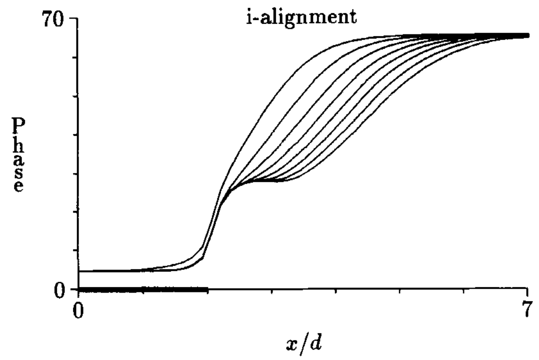

FIGURE 11 Phase-profiles (in°/μm) for o- and i-alignment, $L/d = 10$, $U = 4, 6, 8, 10, 12, 14, 16, 18$ (from left to right) $\Delta n = 0.1$. The location of the electrode is marked on the x-axis.

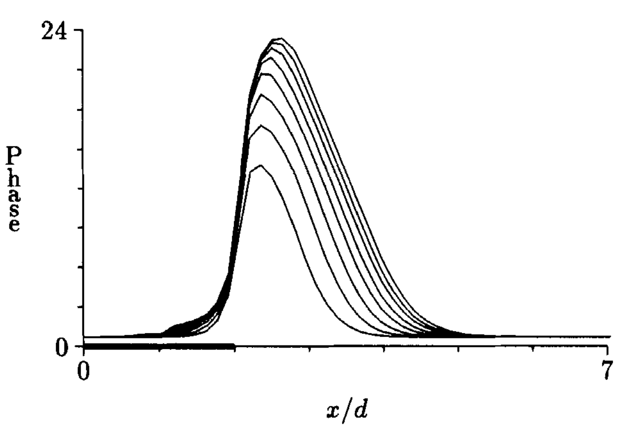

FIGURE 12 Phase profile (in°/μm) for the second optical mode (polarization perpendicular to the director at the boundaries) and o-alignment, $L/d = 10$, $U = 4, 6, 8, 10, 12, 14, 16, 18$.

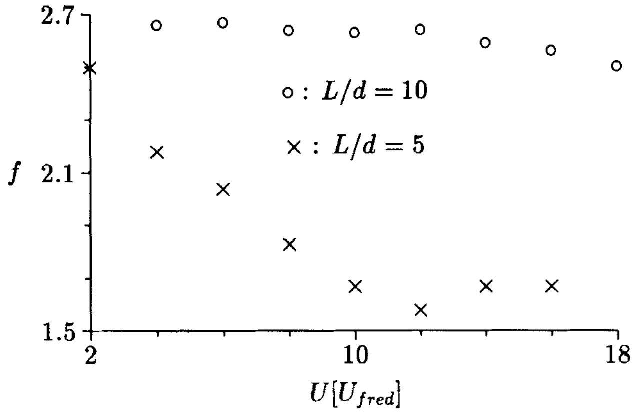

FIGURE 13 Ratio of focal length over aperture, f, as a function of the applied voltage for the o-aligned microlens, $\Delta n = 0.2$, $d = 100\ \mu m$.

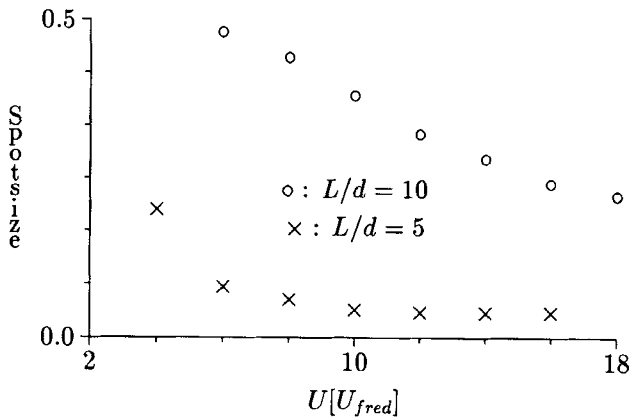

FIGURE 14 Ratio of the spot-size over aperture in the focus-point as a function of the applied voltage for the o-aligned microlens, $\Delta n = 0.2$, $d = 100\ \mu m$.

lens because in this geometry the diameter can be chosen larger than the width of the slit as discussed above. The profiles for the o-alignment clearly have a better shape than the profiles for the i-aligned case. Additionally the o-alignment has the advantage that no formation of disclinations occurs and that a tilt angle can be applied without destroying the symmetry.

Figure 12 shows the phase-profile for the o-aligned lens where the incident light is polarized perpendicular with respect to the director at the boundaries. Because of the mode coupling we have a phase chance near the edges of the electrode which creates a profile with defocussing properties. The focussing properties can therefore be changed from focussing to defocussing by rotating the direction of polarization.

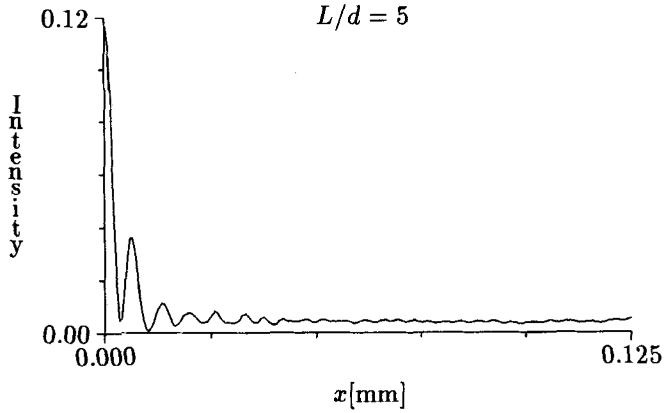

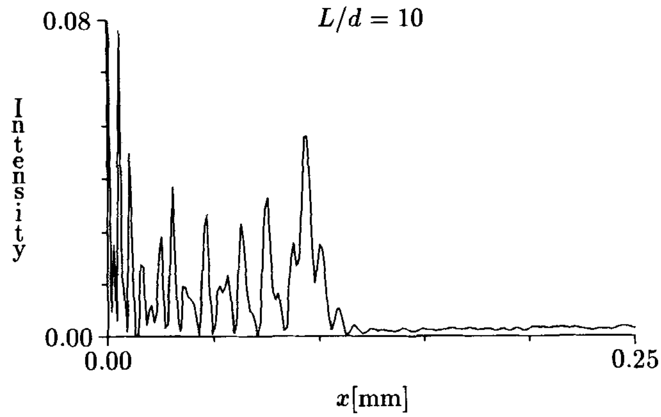

FIGURE 15 Intensity profile of the spot in the focus point at maximum voltage.

Finally, we calculated the optical properties of the o-aligned device from the phase-profiles with the scalar diffraction-theory.[11] For this, we assumed a birefringence of the LC material of $\Delta n = 0.2$ and a cell thickness of 100 μm which results in an effective aperture of 0.5 mm for $L/d = 5$ and 1 mm for $L/d = 10$, respectively. Figure 13 shows the relative focal length of the device and Figure 14 the relative spot-size of the beam at the focus-point as a function of the applied voltage. Figure 15 shows a typical intensity profile at the focus-point. From the figures it is obvious that the plateau in the phase-profile for $L/d = 10$ increases the spot-size at the focus-point and disables the possibility of changing the focal length by changing the applied voltage. The device with $L/d = 5$ possesses relatively good focussing properties but has a lower aperture. Therefore, the optimum L/d-ratio for a cylindrical lens will be somewhere between 5 and 10.

Acknowledgment

We would like to thank A. Kilian from Technical University of Berlin for many helpful discussions.

References

1. T. Nose, and S. Sato, A Liquid Crystal Microlens Obtained with a Non-Uniform Electric Field. *Liq. Crystals*, **5**, 1425 (1989).
2. S. T. Kowel, D. S. Cleverly and P. G. Kornreich, Focusing by Electrical Modulation of Refraction in a Liquid Crystal Cell. *Appl. Optics*, **23**, 278 (1984).
3. M. W. Fritsch, H. Wöhler, G. Haas and D. A. Mlynski, A Liquid Crystal Phase Modulator for Large-Screen Projection. *IEEE Trans. Electron Devices*, **36**, 1882 (1989).
4. G. Haas, S. Siebert and D. A. Mlynski, Simulation of Inhomogeneous Electric Field Effects in Liquid Crystal Displays. *Proc. 9th Int. Display Research Conference, Kyoto*, 524 (1989).
5. A. Kilian and S. Hess, Derivation and Application of an Algorithm for the Numerical Calculation of the Local Orientation of Nematic Liquid Crystals. *Z. Naturforsch.*, **44a**, 693 (1989).
6. G. Haas, M. W. Fritsch, H. Wöhler and D. A. Mlynski, Simulation of Reverse-Tilt Disclinations in LCDs. *SID 90 Digest, Las Vegas*, 102 (1990).
7. G. Haas, H. Wöhler, M. W. Fritsch and D. A. Mlynski, Simulation of Two-Dimensional Director Structures in Twisted Nematic Liquid Crystal Displays. *Proc. 10th Int. Display Research Conference, Amsterdam*, P18 (1990).
8. W. H. Press, B. P. Flannery, S. A. Teukolsky and W. T. Vetterling, *Numerical Recipes*. Cambridge University Press, Cambridge (1988).
9. J. F. Clerc, M. Aizawa, S. Yamauchhi and J. Duchene, Highly Multiplexed Super Homeotropic LCD. *Proc. 9th Int. Display Research Conference*, 188 (1989). S. Yamauchi, M. Aizawa, J. F. Clerc, T. Uchida and J. Duchene, Homeotropic Alignment Fullcolor LCD. *SID 89 Digest*, 378 (1989).
10. R. C. Jones, A New Calculus for the Treatment of Optical Systems I. Description and Discussion of the Calculus. *J. Opt. Soc. Am.*, **31**, 488 (1941).
11. J. W. Goodman, *Introduction to Fourier Optics*. McGraw-Hill, New York (1988).